Ferromagnetic Resonance in Coupled Magnetic Multilayer Systems

Philip E. Wigen and Zhenyong Zhang
Department *of* Physics, The Ohio State *University*
Columbus, Ohio *43210*

Received Octobcr 19, 1992

Ferromagnetic resonance provides a unique technique to evaluate tlie strength of interlayer exchange coupling between ferromagnetic layers separated by "non-magnetic" layers in magnetic multilayer structures as well as the internal magnetic energies within eacli magnctic layers. The dispersion relations, which are sensitive to both the effective uniaxial anisotropy energy and tlie interlayer exchange coupling constant A_{12}, have bcen calculated for systems consisting of two identical ferromagnetic layers eitlier parallel or anti-parallel coupled through a "non-magnetic" spacer. The extcnsions of these calculations to asymmetric structures and/or multilayer structures are discussed. Ferromagnetic resonance techniques have been applied to many magnetic multilayer structures and several results will be reviewcd.

I. Introduct ion

Multilayered structures constructed by alternating layers of ferromagnetic materials, sucli as Co, Fe, Ni and Permalloy, and separated by nominally "non-magnetic" materials have received much attention in the past several years. These nominally "non-magnetic" materials include the noble metals, Ag, Au and Cu, and in addition non-ferromagnetic materials sucli as Pt, Pd, Cr, and Ru. Recent advances in sample preparation techniques, such as molecular beam epitaxial methods (MBE) have nade it possible to produce a large variety of magnet c layered structures with repeatable magnetic propert es. Tlie interest lias been concentrated on tlie novel magnetic behaviors which have only been observed for films with layer thicknesses on the order of scvcral atomic layers, as well as tlie possibility of fabricating new materials for practical applications. In tlie early work on a Fe/Cr structure[1,2], a clear-cut antiparallel coupling between the adjacent Fe layers was observed. Further investigations on the same structure revealed an oscillation behavior between parallel and antiparallel coupling as a function of tlie Cr thickness[3]. For tlie applicatcn interest, this series also exhibits a giant magnetoresistance due to the change in the conduction electron scattering mechanisms as tlie orientation of the magnetization is modified by the application of an external magnetic field[4]. In the Co/Pt or Co/Pd multilayer structures[5,6], the internal uniaxial anisotropy encrgy was significantly enhanced with the decrease of the Co thickness. Samples with perpendicular magnetic anisotropy were reported as the Co thickness was reduced below ~ 15 Å. Another important property of this series was the cnhancement of the magneto-Kerr effect at shorter wave-length whicli increased the interest on Co/Pt and Co/Pd multilayer structures as a prominent perpendicular magneto-optical recording media.

In each case, these unusual characteristics are due to a significant modification of tlie internal energies of the magnetic multilayer structures, especially tlie uniaxial anisotropy energy developed from tlie interface between the magnetic/"non-magnetic" layer and tlie interlayer exchange energy between two adjacent ferromagnetic layers through "non-magnetic" spacers. As will be shown in this paper, magnetic resonance is a useful technique to investigate these magnetic properties. In the ferromagnetic resonance (FMR) experiment, the position of the uniform precessing resonance mode is sensitive to the magnetic anisotropy energy, the magnetostatic energy and tlie Zeeman energy. The variation of tlie uniform mode as a function of tlie orientation of tlie applied field can, in general, separate the contributions from different energy terms. In addition to the uniform mode, there are high order spin-wave modes corresponding to the rf magnetization having eitlier an amplitude or a phase difference from one magnetic layer to the next. Since an extra exchange energy term is involved in the internal energies, the shift of the spin-wave modes from the uniform mode will provide an evaluation of the interlayer exchange coupling strength.

In section II, the theory of the coupled ferromagnetic film resonance (CFFR) will be introduced. As a special example, the theory will be applied to a system consisting of two identical ferromagnetic layers separated by a "non-magnetic" layer. The parallel and anti-

parallel interlayer excliange coupling will be considered separately witli tlie applied external field along both tlie parallel and normal orieiitations to the film plane.

In section III, some experimental results of tlie multilayer structurcs will be discussed. Since tlie range of variables tliat can be clioscn for a given structure is very broad and each structure will have its own unique set of material parameter, it is difficult to "catalog" all tlic data available from tlie various magnetic resonance experiments.

A technique tliat obtains complimentary information to CFFR is Brillouin liglit scattering in which an incoming liglit wave scatters off tlie structure and excites or absorbs tlie same magnetic excitations as observed in tlie magnetic resonance process. Instead of sweeping tlie magnetic field at a constant frequency in CFFR, tlie resonance condition is achieved by "sweeping" frequencics at constant applied field in Brillouin light scattering experiment. Details about tlie experimental set-up aiid results were givcn in tlie literatures[1,2,7–12].

II. Rcsonance Condition

II.1. Gcneral Consideration

When a ferromagnetic material is placed in an applied static magnetic field, tlie magnetic moments in tlic material, if perturbed from their equilibrium orientation, will precess around their equilibrium direction due to tlie torque which can be expressed in terms of either an effective internal field $\mathbf{H}_{eff}$ or a gradient of tlic expression for tlie energy density, I , such tliat,

$$\frac{1}{\gamma}\frac{d\mathbf{M}}{dt} = -\mathbf{M}\times\mathbf{H}_{eff} = \mathbf{M}\times\nabla_M\mathcal{E}\,, \qquad (1)$$

where γ is tlie gyromagnetic ratio and M is tlie magnctization. Tlie equation of motion can be solved by using tlie coordinate systcm show in Figure 1 in which tlie small deviations from equilibrium are in tlie $\hat{\mathbf{e}}_\theta$ and $\hat{\mathbf{e}}_\phi$ directions. This orientation of the coordinate system is used in order tliat tlie dispersion relatiori can be obtained as a function of tlie orientation of M from a direction normal to the film to one lying in the film plane. In this coordinate system the magnetization has tlie form

$$\mathbf{M} = M_0\hat{\mathbf{e}}_\mathbf{r} + m_\phi\hat{\mathbf{e}}_\phi + m_\phi\hat{\mathbf{e}}_\phi, \qquad (2)$$

wliere m_θ and m_ϕ are the small transverse components of tlie magnctization associated witli tlic precession, $m_\theta = M\delta\theta$, $m_\phi = Msin\theta\delta\phi$ and 60 and 64 are small deviations from the equilibrium direction.

In tlie system witli N ferromagnetic layers separated by "non-magnetic" layers but coupled by an exchange iiiteraction, it is convenient to use the encrgy per film arca E instead of volume energy density $\mathcal{E}$:

$$E = \sum_{i=1}^{N} t_i\mathcal{E}_i - \sum_{i=1}^{N-1} A_{i,i+1}\frac{\mathbf{M}_i\cdot\mathbf{M}_{i+1}}{M_iM_{i+1}}\,, \qquad (3)$$

wliere t_i and $\mathcal{E}_i$ are tlie thickness and energy density of tlie ith layer, and $A_{i,i+1}$ is the exchange energy per unit surface area between tlie itli and (i + 1)th layers. Tlie negative sign is clioscn so tliat $A_{i,i+1}$ will be positive for parallel coupled systcm and negative for anti-parallel system.

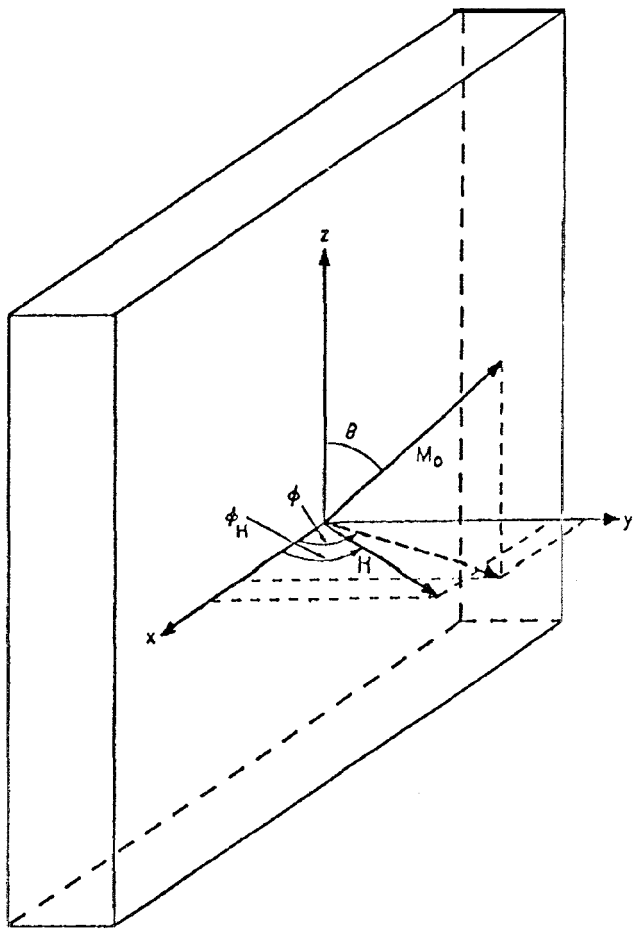

Figure 1: Tlie coordinate systcm uscd for tlie evaluation of tlie CFFR condition.

Tlie resonance equation (1) will have tlie new form:

$$\frac{1}{\gamma_i}\frac{d\mathbf{M}_i}{dt} = \mathbf{M}_i\times\left(\frac{1}{t_i}\nabla_{M_i}E\right)\,, \qquad (i = 1,2,....,N)\,. \qquad (4)$$

In tlie equilibrium orientation, the magnctization will not have a variation in either time or space across each magnetic layer and Eq. (4) reduces to

$$\mathbf{M}_i\times\frac{1}{t_i}\nabla_{M_i}E = \frac{1}{t_i}\left(E_{\theta_i}\hat{\mathbf{e}}_{\phi_i} - \frac{E_{\phi_i}}{sin\theta_i}\hat{\mathbf{e}}_{\theta_i}\right) = 0\,, \qquad (5)$$

where the notation $E_{\theta_i} = \partial E/\partial\theta_i$ and $E_{\phi_i} = \partial E/\partial\phi_i$ is used.

The equations of motion are linearized by expanding Eq. (4) about tlie equilibrium orientation and retaining only terms to the first order of m_{θ_i} and m_{ϕ_i} expressed in Eq. (2). In linearized form the equations of motion become a set of $2N$ equations:

$$
\begin{aligned}
\frac{1}{\gamma_1}\frac{d}{dt}m_{\theta_1} &= -\frac{1}{t_1 M_1 sin\theta_1}\left(E_{\theta_1\phi_1}m_{\theta_1}+\frac{E_{\phi_1\phi_1}}{sin\theta_1}m_{\phi_1}\right)-\frac{1}{t_1 M_2 sin\theta_1}\left(E_{\theta_2\phi_1}m_{\theta_2}+\frac{E_{\phi_1\phi_2}}{sin\theta_2}m_{\phi_2}\right),\\
\frac{1}{\gamma_1}\frac{d}{dt}m_{\phi_1} &= \frac{1}{t_1 M_1}\left(E_{\theta_1\theta_1}m_{\theta_1}+\frac{E_{\theta_1\phi_1}}{sin\theta_1}m_{\phi_1}\right)+\frac{1}{t_1 M_2}\left(E_{\theta_1\theta_2}m_{\theta_2}+\frac{E_{\theta_1\phi_2}}{sin\theta_2}m_{\phi_2}\right),\\
\frac{1}{\gamma_i}\frac{d}{dt}m_{\theta_i} &= -\frac{1}{t_i M_i sin\theta_i}\left(E_{\theta_i\phi_i}m_{\theta_i}+\frac{E_{\phi_i\phi_i}}{sin\theta_i}m_{\phi_i}\right)-\frac{1}{t_i M_{i+1} sin\theta_i}\left(E_{\theta_{i+1}\phi_i}m_{\theta_i+1}+\frac{E_{\phi_i\phi_{i+1}}}{sin\theta_{i+1}}m_{\phi_{i+1}}\right)\\
&\quad -\frac{1}{t_i M_{i-1} sin\theta_i}\left(E_{\theta_{i-1}\phi_i}m_{\theta_{i-1}}+\frac{E_{\phi_{i-1}\phi_i}}{sin\theta_{i-1}}m_{\phi_{i-1}}\right) \qquad (i=2,....,N-1),\\
\frac{1}{\gamma_i}\frac{d}{dt}m_{\phi_i} &= \frac{1}{t_i M_i}\left(E_{\theta_i\theta_i}m_{\theta_i}+\frac{E_{\theta_i\phi_i}}{sin\theta_i}m_{\phi_i}\right)+\frac{1}{t_i M_{i+1}}\left(E_{\theta_i\theta_{i+1}}m_{\theta_{i+1}}+\frac{E_{\theta_i\phi_{i+1}}}{sin\theta_{i+1}}m_{\phi_{i+1}}\right)\\
&\quad +\frac{1}{t_i M_{i-1}}\left(E_{\theta_{i-1}\theta_i}m_{\theta_{i-1}}+\frac{E_{\theta_i\phi_{i-1}}}{sin\theta_{i-1}}m_{\phi_{i-1}}\right) \qquad (i=2,....,N-1),\\
\frac{1}{\gamma_N}\frac{d}{dt}m_{\theta_N} &= -\frac{1}{t_N M_N sin\theta_N}\left(E_{\theta_N\phi_N}m_{\theta_N}+\frac{E_{\phi_N\phi_N}}{sin\theta_N}m_{\phi_N}\right)-\\
&\quad \frac{1}{t_N M_{N-1} sin\theta_N}\left(E_{\theta_{N-1}\phi_N}m_{\theta_{N-1}}+\frac{E_{\phi_{N-1}\phi_N}}{sin\theta_{N-1}}m_{\phi_{N-1}}\right),\\
\frac{1}{\gamma_N}\frac{d}{dt}m_{\phi_N} &= \frac{1}{t_N M_N}\left(E_{\theta_N\theta_N}m_{\theta_N}+\frac{E_{\theta_N\phi_N}}{sin\theta_N}m_{\phi_N}\right)+\\
&\quad \frac{1}{t_N M_{N-1}}\left(E_{\theta_{N-1}\theta_N}m_{\theta_{N-1}}+\frac{E_{\theta_N\phi_{N-1}}}{sin\theta_{N-1}}m_{\phi_{N-1}}\right), \qquad (6)
\end{aligned}
$$

where $E_{\theta_i\theta_j} = \partial^2 E/\partial\theta_i\partial\theta_j$, $E_{\phi_i\phi_j} = \partial^2 E/\partial\phi_i\phi_j$ and $E_{\theta_i\phi_j} = \partial^2 E_i'\partial\theta_i\partial\phi_j$.

Eq. (6) can be expressed in matrix form[13,14] with the roots of the determinant giving the resonance frequencies of the multilayer system. In general N modes at different frequencies will be obtained for a given applied field. In the case that the N magnetic layers are identical and not coupled with their adjacent layers, those N modes will be degenerate and the dispersion relation will be the same as that of a single magnetic layer system. The ellipticity of the precession, m_{θ_i}/m_{ϕ_i}, and, in the case of coupled layers, the phase shift from one layer to another can also be obtained from the eigenvector (m_{θ_1}, m_{ϕ_1}, ..., me,, $m_{\phi N}$) corresponding to each mode.

The internal energies $\mathcal{E}_i$ that normally contribute to the resonance equations (6) are the following:

a. Zeeman Energy

In the presence of an applied magnetic field $\mathbf{H}_0$, the energy expression is given as

$$
\begin{aligned}
\mathcal{E}_i^z &= -\mathbf{H}_0\cdot\mathbf{M}_i = -H_0 M_i[cos\theta_H cos\theta_i\\
&\quad + sin\theta_H sin\theta_i cos(\phi_i-\phi_H)], \qquad (7)
\end{aligned}
$$

where θ_H and ϕ_H are the orientation angles of the applied external field $\mathbf{H}_0$.

b. Cubic Crystalline Anisotropy Energy

In this contribution the crystalline anisotropy energy will be considered for the condition that all three unique axes in the cubic structure may be oriented normal to the film, [001], [110] and [111]. For a [001] oriented film the energy expression has the form

$$
\begin{aligned}
\mathcal{E}^c_{[001],i} &= \frac{K_{1,i}}{M_i^4}(M_{x,i}^2M_{y,i}^2+M_{y,i}^2M_{z,i}^2+M_{z,i}^2M_{x,i}^2)\\
&\quad + \frac{K_{2,i}}{M_i^6}M_{x,i}^2M_{y,i}^2M_{z,i}^2\\
&= K_{1,i}\left(\frac{sin^4\theta_i sin^2 2\phi_i}{4}+\frac{sin^2 2\theta_i}{4}\right)\\
&\quad + K_{2,i}\frac{sin^2\theta_i sin^2 2\theta_i sin^2 2\phi_i}{16}. \qquad (8)
\end{aligned}
$$

For a [110] oriented film the energy expression has the form (x || [001])

$$\begin{aligned}\mathcal{E}^c_{[110],i} &= \frac{K_{1,i}}{M_i^4}\left(M_{x,i}^2M_{y,i}^2+M_{x,i}^2M_{z,i}^2+\frac{M_{y,i}^4}{4}+\frac{M_{z,i}^4}{4}-\frac{M_{y,i}^2M_{z,i}^2}{2}\right)\\ &\quad+\frac{K_{2,i}}{M_i^6}\left(\frac{M_{x,i}^2M_{y,i}^4}{4}+\frac{M_{x,i}^2M_{z,i}^4}{4}-\frac{M_{x,i}^2M_{y,i}^2M_{z,i}^2}{2}\right)\\ &= K_{1,i}\left(\frac{sin^4\theta_i sin^2 2\phi_i}{4}+\frac{sin^2\theta_i cos^2\phi_i}{4}+\frac{sin^4\theta_i sin^4\phi_i}{4}+\frac{cos^4\theta_i}{4}-\frac{sin^2 2\theta_i sin^2\phi_i}{8}\right)\\ &\quad+K_{2,i}\left(\frac{sin^6\theta_i sin^2\phi_i sin^2 2\phi_i}{16}+\frac{sin^2 2\theta_i cos^2\theta_i cos^2\phi_i}{16}-\frac{sin^2\theta_i sin^2 2\theta_i sin^2 2\phi_i}{32}\right).\end{aligned} \tag{9}$$

For a [111] orieiitcd film tlie energy expression Iias the form (x || [$\bar{1}\bar{1}$2])

$$\begin{aligned}\mathcal{E}^c_{[111],i} &= \frac{K_{1,i}}{M_i^4}\left(\frac{M_{x,i}^4}{4}+\frac{M_{y,i}^4}{3}+\frac{M_{z,i}^4}{4}+\frac{M_{x,i}^2M_{z,i}^2}{2}+\frac{\sqrt{2}}{3}M_{x,i}^3M_{y,i}-\sqrt{2}M_{x,i}M_{y,i}M_{z,i}^2\right)\\ &\quad+\frac{K_{2,i}}{M_i^6}\frac{(\sqrt{2}M_{x,i}-M_{y,i})^2[(M_{x,i}+\sqrt{2}M_{y,i})^2-3M_{z,i}^2]^2}{108}\\ &= K_{1,i}\left(\frac{sin^4\theta_i cos^4\phi_i}{4}+\frac{sin^4\theta_i sin^4\phi_i}{3}+\frac{cos^4\theta_i}{4}+\frac{sin^2 2\theta_i cos^2\phi_i}{8}\right.\\ &\quad\left.+\frac{\sqrt{2}}{3}sin^4\theta_i sin\phi_i cos^3\phi_i-\frac{\sqrt{2}}{8}sin^2 2\theta_i sin 2\phi_i\right)\\ &\quad+K_{2,i}\frac{sin^2\theta_i(\sqrt{2}cos\phi_i-sin\phi_i)^2[sin^2\theta_i(cos\phi_i+\sqrt{2}sin\phi_i)^2-3cos^2\theta_i]^2}{108}.\end{aligned} \tag{10}$$

c. Uniaxial anisotropy energy

Iii addition to tlie demagnetization encrgy producing an casy plane material, a uniaxial anisotropy encrgy can be introduced iiito tlie material if it Iias hexagonal symmetry with tlic c-axis normal to tlic plane or if an induced uniaxial anisotropy energy is present due to strains developed during growth or iii the case of nlloy films, a regular variation iii tlie position of certain ions iii tlic lattice producing a growth iiiduced anisotropy energy. To the fourth order of $M_{y,i}$ tlie form for the ciicrgy expression will be;

$$\mathcal{E}_{u,i} = -K_{2u,i}^{eff}\frac{M_{y,i}^2}{M_i^2}-K_{4u,i}\frac{M_{y,i}^4}{M_i^4} = -K_{2u,i}^{eff}sin^2\theta_i sin^2\phi_i - K_{4u,i}sin^4\theta_i sin^4\phi_i\,. \tag{11}$$

The first term in Eq. (11) will include the demagnetization encrgy $2\pi M_{y,i}^2$ and tlic internal uniaxial aiiisotropy eiiergy $-K_{2u,i}M_{y,i}^2/M_i^2$ following the relation;

$$K_{2u,i}^{eff} = K_{2u,i} - 2\pi M_i^2\,. \tag{12}$$

d. Surface aiiisotropy energy

One of the important contribution to the uniaxial aiiisotropy cnergy $K_{2u,i}$ comes from the surface anisotropy[5,15–19]. Ii$_1$ the case where a magnetic layer has a thickness grenter tlian the magnetic correlation length, which is oii tlie order of a few hundred Angstroms, tlic presence of a surface aiiisotropy energy,

K_{sur}, will influence the resonance condition of the surface spins and produce a "pinned" boundary condition that gives rise to standing spin-wave modes that can be excited across the thickness of the film[13]. In the case of typical multilayer films, the film thicknesses are on the order of 10 Å and the excitation energy of the higher order spin-waves associated with a single layer would be so large, on the order of 10^2 tesla, that they will not be observed in the CFFR experiment. As a result the surface anisotropy energy, instead of affecting only the surface of each film, will be weighted over the film thickness to produce an effective volume anisotropy energy having the form

$$K_{2u,i} = K^b_{2u,i} + 2K_{sur,i}/t_i \ , \qquad (13)$$

where $K^b_{2u,i}$ is the bulk uniaxial anisotropy energy and the factor of 2 in the second term arises from the two surfaces acting on each layer.

Another contribution to the energy density $\mathcal{E}_i$ comes from the direct exchange interaction between magnetic spins within each layer. However, as will be shown later, the strength of the exchange interaction between two magnetic layers, A_{12}, is much smaller ($10^{-3} \sim 10^{-2}$) than that within the ferromagnetic layer itself. As a result in the normal CFFR modes, the rf magnetization vectors in each individual ferromagnetic layers are nearly uniform across the film but they can have both a phase and an amplitude difference from one ferromagnetic layer to the next[18]. As a result, to first order each layer is treated as a continuous media with a uniform magnetization $\mathbf{M}_i$. In some multilayer system for which the magnetic layer thickness is on the order of 100 ~ 1000 Å, the contribution from the exchange interaction within each layer may not be negligible. In this case the calculations must include the spin-wave energy within each layer as reported in the literature[11,12,20–22].

c. In-plane anisotropy energy

In the case of the anti-parallel coupled films, an in-plane uniaxial anisotropy energy, in addition to that having a unique direction normal to the structure, will produce a unique axis in the plane of the film. Two orientations of the applied magnetic field will be of interest for our purpose. One will be with the easy axis parallel to the x-axis and the form of the energy expression will be

$$\mathcal{E}^x_{D,i} = -D^x_i M^2_{x,i}/M^2_i = -D^x_i sin^2\theta_i cos^2\phi_i \qquad (14)$$

and the other will be with the easy axis parallel to z-axis and the form will be

$$\mathcal{E}^z_{D,i} = -D^z_i M^2_{z,i}/M^2_i = -D^z_i cos^2\theta_i \ , \qquad (15)$$

where D^x_i and D^z_i are the in-plane anisotropy energy constants for which the easy axis is along the x-axis or the z-axis respectively when the D values are positive.

f. Linewidth and damping parameters

The linewidth in the CFFR spectrum is relatively broader than that of a single ferromagnetic film. One of the most important contribution to the linewidth may be due to the inhomogeneities in the internal fields of the sample[23]. These inhomogeneities may arise from non-homogeneous stresses in the film or any variation in the layer thickness from layer to layer or the fluctuation of the interlayer diffusion between the ferromagnetic and "non-magnetic" layers.

Another contribution, when the inhomogeneities do not dominate, is the spin relaxation processes in the multilayer films. Relaxation terms cannot be included directly into the energy expression and must be added to the right hand side of the equations of motion, Eq.(4), as a phenomenological damping term. The damping term in the Gilbert form is

$$-\frac{\alpha}{\gamma_i M_i}\mathbf{M}_i \times \frac{d}{dt}\mathbf{M}_i \ , \qquad (16)$$

where α is the damping parameter. This phenomenological term predicts a symmetric Lorentz shape absorption line with the linewidth $\Delta H = 2\omega\alpha/\gamma_i$ if the ith layer is not coupled with the other layers[14].

The intensity of the CFFR modes is sensitive to both the amplitude and the phase variation from one layer to another. In the microwave resonance, the rf pumping field has a space variation, on the order of 1 cm, much larger than the sample's dimension which is on the order of 1 mm. As a result the rf field across the film surface can be treated as a uniform field which only varies as a function of time. Assuming that the direction of the rf field is always parallel to the z direction and $\mathbf{M}_i$ stays in the x-y plane (i.e. $\theta_i = \pi/2$) the intensity of each mode will have the relation[14,24]

$$I \propto \left(\sum_{i=1}^{N} t_i m_{\theta,i}\right)^2 / \sum_{i=1}^{N} t_i (m^2_{\theta,i} + m^2_{\phi,i}). \qquad (17)$$

In the next part, a ferromagnetically coupled ($A_{i,j} > 0$) trilayer system, which includes two ferromagnetic layers separated by a "non-magnetic" layer, will be considered.

II.2. Parallel Coupled Trilayer System

In the trilayer system, the internal energy density for each layer , $\mathcal{E}_1$ and $\mathcal{E}_2$ may include any of the energy terms in Eq. (7) through Eq. (15). As observed in the previous section, the details of the internal energies have a profound effect on the positions of the resonance. However, for the purpose of illustration in this section, the forms of the energy to be used in the analysis will be limited to the Zeeman energy with the external field $\mathbf{H}_0$ in the x-y plane, the effective uniaxial

anisotropy energy liaving a uniqiie direction normal to tlie place (y-axis) and the interlayer excliange energy. Tlie calculation including tlie cubic anisotropy energy can be found in the literature[12,23,25]. The energy per unit area will tlien have the form:

$$\begin{aligned} E &= -\mathbf{H}_0 \cdot (t_1\mathbf{M}_1 + t_2\mathbf{M}_2) - \left(t_1 K_{2u,i}^{eff} \frac{M_{y,1}^2}{M_1^2} + t_2 K_{2u,2}^{eff} \frac{M_{y,2}^2}{M_2^2} \right) - A_{12} \frac{\mathbf{M}_1 \cdot \mathbf{M}_2}{M_1 M_2} \\ &= -H_0[t_1 M_1 sin\theta_1 cos(\phi_1 - \phi_H) + t_2 M_2 sin\theta_2 cos(\phi_2 - \phi_H)] - t_1 K_{2u,1}^{eff} sin^2\theta_1 sin^2\phi_1 \\ &\quad -t_2 K_{2u,2}^{eff} sin^2\theta_2 sin^2\phi_2 - A_{12}[cos\theta_1 cos\theta_2 + sin\theta_1 sin\theta_2 cos(\phi_1 - \phi_2)]. \end{aligned} \tag{18}$$

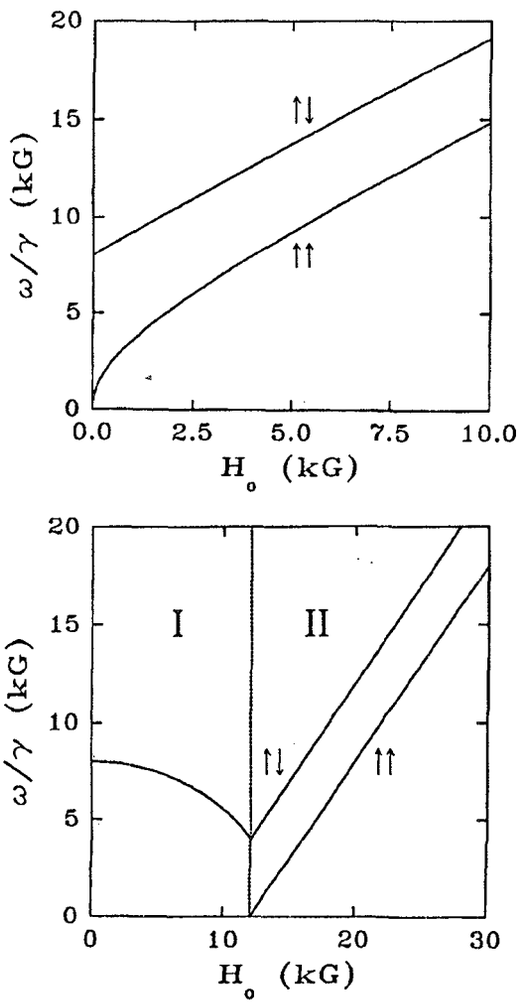

Figure 2: The dispersion relations for a. system consisting of two identical parallel coupled ferromagnetic layers with the external field applied top) in tlie plane of tlie film; bottom) normal to the film plane. The values of parameters used in tliis figure are $H_u = -12$ kG and $H_{ex} = 2.0$ kG. The ↑↑ represents the acoustic mode and ↑↓ is the optical mode.

Tlie equilibrium orieiitation of the magnetization in eacli layer can be obtained from **Eq.** (5). For an easy plane material, $K_{2u,i}^{eff} < 0$, when tlie magnetic field is applied in the plane of the structure along tlie **x**-axis, tlie magnetization in botli layers will be oriented along the direction of tlie applied field. Tlius tlie hysteresis loop for tlie coupled system will be tlie same as tliat for the uncoupleù system in this geometry.

When the magnetic field is applied normal to tlie film, y-axis, tlie applied field must work against tlie torque induced by the uniaxial/demagnetization energy. In tlie case tliat tlie two ferromagnetic layers have different effective anisotropy fields $H_{u,i} = 2K_{2u,i}^{eff}/M_i$, tlie magiietization in eacli film will not always be parallel to eacli otlier below tlie saturation field. As a result tlie applied field must also work against tlie torque induced by the interlayer excliange encrgy, A_{12}. Only when $H_{u,1} = H_{u,2} = H_u$, the equilibrium orientation of $\mathbf{M}_1$ will always be parallel to $\mathbf{M}_2$ and independent of tlie exchange energy. Tlie y-compoiient of tlie magnetization in tliis case will have a simplified form

$$M_y = M(-H_0/H_u) \tag{19}$$

and the film becomes saturated when $H_0 = -H_u$. Again tliis equilibrium orientation is tlie same condition expected for a single ferromagnetic film.

The dispersion relations can be obtained from Eq. (6) by letting N = 2 and assuming that tlie response of the rf magnetization is of the form $exp(i\omega t)$. **A** typical example of the dispersion curve, ω/γ, versus tlie applied magnetic field, H_0 is shown in Figure 2 at both tlie parallel orientation, $\mathbf{H}_0$ || x and the perpendicular orientation, $\mathbf{H}_0 \parallel$ y assuming tliat the properties of tlie two ferromagnetic layers are identical (i.e. $M_1 = M_2 = M$, $H_{u,1} = H_{u,2} = H_u$ and $t_1 = t_2 = t$). One of tlie inodes will have tlie magnetization in eacli film precessing in phase witli the same amplitude ($m_{\theta,1} = \boldsymbol{me}$, ~ and $m_{\phi,1} = m_{\phi,2}$), tlie acoustic mode (↑↑), and tlie dispersion relation is tlie same as tliat for tlie individual ferromagnetic layers as if they were to remain uncoupled

$$\frac{\omega}{\gamma} = \sqrt{H_0(H_0 - H_u)} \qquad (\mathbf{H}_0 \parallel \mathbf{x})$$

and (20)

$$\frac{\omega}{\gamma} = H_0 + H_u \quad (H_0 > -H_u) \quad (\mathbf{H}_0 \,||\, \mathbf{y}) \quad (21)$$

Iii tlie otlier mode, the rf magnetization of tlie two layers will precess witli tlie same amplitude but in tlie opposite direction ($m_{\theta,1} = -m_{\theta,2}$ and $m_{\phi,1} = -m_{\phi,2}$), tlie optical rnode ($\uparrow\downarrow$). The frequency of tlie optical mode is sliifted to a liiglier value due to tlie additional torque introduced from tlie excliange coupling term because tlie magnetization in each individual layers is not oriented parallel to eacii otlier during the precession. Tlie dispersion relation in the saturation region will have tlie same form as in Eq. (20) if tlie external field, H_0, is rcplaced by H_0+2H_{ex}, wliere tlie excliange field is defined as $H_{ex} = A_{12}/tM$. Below tlie saturation region with tlie app'ied field normal to the film, the resonance frequency of the optical mode remains at high values and decreases witli the increase of tlie field. Tlie dispersion relation of tlie optical mode in this region will be

$$\omega/\gamma = \sqrt{2H_{ex}(2H_{ex} - H_u + H_0^2/H_u)}\,. \quad (22)$$

Tlie intensity of each mode can be calculated from Eq. (17). The acoustic mode will have a large intensity while tlie intensity of tlie optical mode will be zero. As a result tlie cptical mode will not be excited by a uniform rf field. One way to overcome tlie difficulty is to make samples with different tliicknesses in each layer. However the intensity of the optic mode will still be zero if the thickness difference between the two layers does not produce a difference of the effective anisotropy field $H_{u,i}$ from one layer to another[7,23], because tlie amplitude of tlie rf magnetization in each layer is inversely proportional to tlie film tliickness. In most systems, the effective uniaxial anisotropy field $H_{u,i}$ will cliange witli the change of tlie film thickness. As mentioned before, one of tlie main contributions to tlie uniaxial anisotropy energy comes from tlie surface anisotropy energy which will produce a $1/t$ dependence of tlie effective field. When tlie magnetic layer tliickness is on the order of 10 Å, tlie change of the effective anisotropy field $H_{u,i}$ (several kG) due to tlie cliange of the film tliickness (several Å) will be large enough to see a weak optic mode on tlie liigh frequency or low magnetic field side of tlie acoustic mode.

11.3 Antiparallel Coupled Ferromagnetic Rilaycr Syste m

In the case of anti-parallel coupling betwcen tlie ferromagnetic layers, tlie sign of tlie exchange coupling coefficient, A_{12}, changes. While this is a subtle change in tlie equations of motion it has a profound effect on tlie equilibrium orientation of the magnetization in tlie two ferromagnetic layers as well as on the dispersion relation.

For two ferromagnetic films coupled anti-parallel and having a uniaxial anisotropy energy normal to the film, $K_{2u}^{eff} < 0$, as well as an in-plane uniaxial anisotropy of tlie form given by Eq. (14), tlie energy density can be expressed as

$$\begin{aligned} E &= -\mathbf{H}_0 \cdot (t_1\mathbf{M}_1 + t_2\mathbf{M}_2) - \left(t_1 K_{2u,1}^{eff}\frac{M_{y,1}^2}{M_1^2} + t_2 K_{2u,2}^{eff}\frac{M_{y,2}^2}{M_2^2}\right) \\ &\quad - \left(D_1^x t_1\frac{M_{x,1}^2}{M_1^2} + D_2^x t_2\frac{M_{x,2}^2}{M_2^2}\right) - A_{12}\frac{\mathbf{M}_1\cdot\mathbf{M}_2}{M_1 M_2} \\ &= -H_0[t_1 M_1 sin\theta_1 cos(\phi_1 - \phi_H) + t_2 M_2 sin\theta_2 cos(\phi_2 - \phi_H)] \\ &\quad -(K_{2u,1}^{eff} t_1 sin^2\theta_1 sin^2\phi_1 + K_{2u,2}^{eff} t_2 sin^2\theta_2 sin^2\phi_2) - (D_1^x t_1 sin\theta_1^2 cos\phi_1^2 \\ &\quad + D_2^x t_2 sin^2\theta_2 cos^2\phi_2) - A_{12}[cos\theta_1 cos\theta_2 + sin\theta_1 sin\theta_2 cos(\phi_1 - \phi_2)]\,. \end{aligned} \quad (23)$$

The external field $\mathbf{H}_0$ is assumed to lie in the $\mathbf{x} - \mathbf{y}$ plane and the exchange coupling constant, A_{12}, is less than zero.

As in the parallel coupled system the equilibrium orientation of the magnetization of each layer can be obtained from Eq. (5). Assuming again that each layer is identical, $M_1 = M_2 = \mathrm{M}$, $K_{2u,1}^{eff} = K_{2u,2}^{eff} = K_{2u}^{eff}$, $t_1 = t_2 = t$ and $D_1^x = D_2^x = \mathrm{D}^{\mathrm{X}}$, the application of the external field along the easy axis ($\mathbf{H}_0 \,||\, \mathrm{x}$) will produce three different sets of conditions for the magnetization. For increasing magnetic field, the first region is in the range $0 \le H_0 \le \sqrt{H_D(2H_{ex} + H_D)} = H_\uparrow$, where $H_D = 2\mathrm{D}^{\mathrm{X}}/M$ is the in-plane anisotropy field and $H_{ex} = |A_{12}|/tM$ is the exchange field acting on each layer. In this field range the magnetization of the films continue to lie along the $\pm$x-axis. At the spin flop

ficlcl for iiicrcasing magnetic fields, $H_0 = H_1$, tlic spiiis reorient toward tlie direction perpendicular to tlic field along tlie $\pm z$-axis but canted toward tlic x-axis at the angle $\theta_1 = \pi - \theta_2 = sin^{-1}[H_0/(2H_{ex} - H_D]$. Iii tlic second rcgion tlic spiiis remain caiitctl until tlic field has reached tlic saturation ficld $H_0 = H_{\|,sat} = 2H_{ex} - H_D$, at which value tlic spiiis lie parallel to tlic x-axis in tlie saturation state. The tliird range of field values is for $H_0 > H_{\|,sat}$ for which tlic magnetization is always aloiig tlie direction of tlie magnetic ficlcl.

For dccrcasiiig magnetic fieid tlic spin flop occiirs at a lower ficld value of $H_\downarrow = \sqrt{H_D(2H_{ex} - H_D)^2/(2H_{ex} + H_D)}$. This rcsiilts in a liystcrcsis about tlic viciiiity of tlie spin-flop field[26]. Tlic magnitude of tlic x component of tlie net magnetization as a function of tlie external ficld applied along tlic x-direction is shown in Figiire 3.

When tlie magnetic field is applicd normal to tlie film, ($\mathbf{H}_0 \parallel$ y), tlie spins are forced to rotate about tlic a-asis toward tlic y-nsis within tlic x-y plane and a spin-flop coiiditioii is iiot observcd. Tlic equilibrium condition from Eq. (5) gives tlic coiiditioii $\phi_1 = \pi - \phi_2 = sin^{-1}[H_0/(2H_{ex} + H_D - H_u)]$. Uiitler these conditions, tlic iict magnetization aloiig tlie y-axis is proportional to the external ficld until tlic applicd ficld rcaclics the saturation value $H_0 = 2H_{ex} + H_D - H_u = H_{\perp,sat}$ above which tlie iict magnetization aloiig tlic ficlcl direction remains saturated at M.

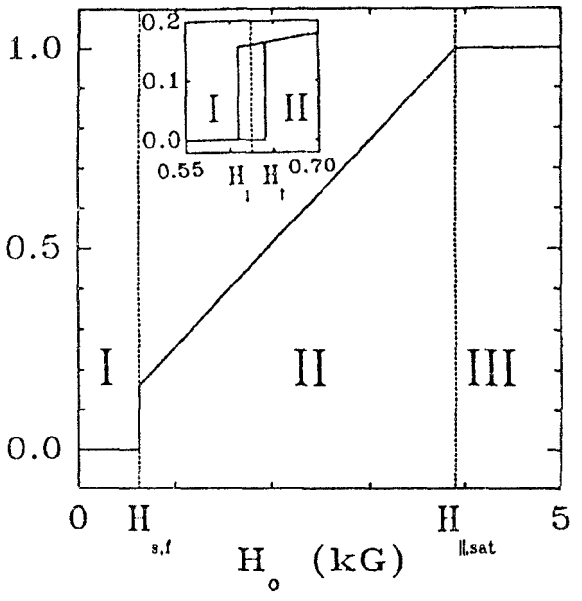

Figure 3: Tlic in-plane component of the magnetization as a fiiiiction of tlie field strength for a pair of anti-parallel coupled ferromagnetic films when tlie applied field is in tlie plane and parallel to tlic in-plane anisotropy field ($\mathbf{H}_0 \parallel$ x-axis). The values of tlie parameters uscd are $H_u = -12$ kG, $H_{ex} = 2.0$ kG arid $H_D = 0.1$ kG. Tlic inset figure shows tlie hysteresis in tlic vicinity of tlic spin-flop field.

Though in tlie casy plane multilayer system, $K_{2u}^{eff} < 0$, only tlic caiitctl and saturation rcgioiis exist in tlic hysteresis loop with tlic external field normal to tlic film, tlic spiii-flop condition can be observed[27] for tlic system with casy axis normal to tlic film, $K_{2u}^{eff} > 0$. In this orientation tlic spins will stay along the $\pm$y-axis until tlic external field is large enough to force tlic spiiis to reorient anti-parallel in tlic film plane but canted toward tlic direction of tlie external ficlcl (y-axis). Because tlic effective uniaxial aiiisotropy field, H_u, is oii tlie ordcr of $1 \sim 10$ kG, tlie separation between tlic spin-flop field with iiicrcasiiig magnetic field, $H_\uparrow$, aiid tliat with dccrcasiiig magnetic ficlcl, $H_\downarrow$, will be oii the ordcr of 1 kG,much larger, than tliat shown iii Figiire 3 for parallcl orientation.

Using tlic form of tlic ciicrgy given in Eq. (22), tlic equation of motion for Llie system as givcii in Eq. (6) can be obtained. For tlic parallcl orientation, $\mathbf{H}_0 \parallel$ x-axis, tlic dispcrsioii relation is shown iii Figure 4. In rcgioii I, below tlic spiii-flop field, tlie dispcrsioii rclatioii is significantly modified from that of a bulk antiferromagnetic material.

In a bulk antiferromagnetic material, tlic dispersion relation is givcii by the equation[28]

$$\frac{w}{\gamma} = \sqrt{H_D(2H_{ex} + H_D)} \pm H_0 \approx \sqrt{2H_{ex}H_D} \pm H_0 , \tag{24}$$

where H_{ex}, is tlic exchange field that arises from tlic exchange interaction between tlie magnetic moments oii tlic two sublattices. Iii most antiferromagnetic materials tlic exchange field is orders of magnitude larger than the anisotropy field, H_D, so tlie approximation iii Eq. (23) is tlic usual expression for dispersion relation. If an external magnetic field is applied along the casy axis dirction, tlic degeneracy of tlic two modes at zcro field is lifted. One mode increases iii frequency while tlic other dccrcascs with tlie field H_0 as indicated iii Eq. (23).

For anti-parallel coupled films tlic situation is quite different in tliat cacli ferromagnetic layer lias Llie added torque duc to tlie magnetostatic ciicrgy contribution. Tlic effect of this added torque is to lift tlie degeneracy in tlie zero field modes as shown iii Figure 4. The low frequency mode decreases to zero frequency while tlic liigli frequency mode iiicrcascs slightly as tlie field approaches to tlie spin-flop field. At tlie spin-flop ficlcl there is a discontinuity in tlic high frequency mode but in addition tlic position of the acoustic modc aiid the optic mode iiitcrcliange regions. As tlic applicd field is further increased in rcgioii II, tlie frequency of tlic acoustic mode iiicrcascs but with a significantly different behavior tliaii tliat observcd for tlie case of a siiiglc layer ferromagnetic film (sce tlic dashed curve in Figure 4). At the same time tlic frcqiiency of tlic optical inodc decreases aiid reaches zero at tlic saturatioii field. Iii tlic saturation region, tlie acoustic mode is degenerate with that of tlie ferromagnetic resonance for a siiiglc

layer while tlie optical inodc is shifted to tlic low frequency or Iiigli magnetic field side by tlic field, $2H_{ex}$. The dispersion relations in each rcgioii are given by tlic following equations:

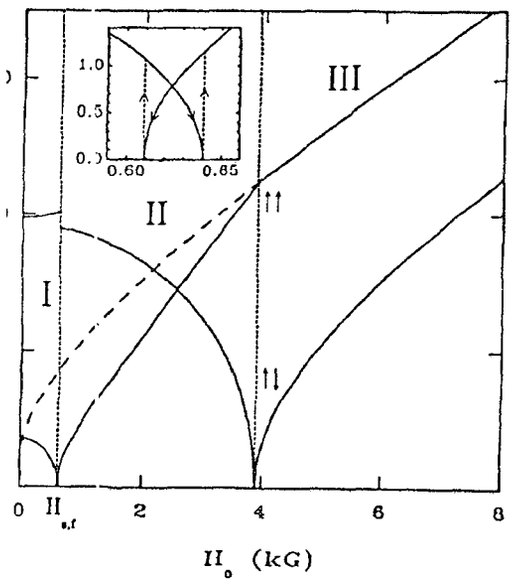

Figure 4: Tlic tlispcrsioii rclatioii for tlic sainc condition ris Figure **3.** The notations of ↑↑ aiid ↑↓ are tlie same as those in Figure 2. The value of $g = 2$ is uscd along with other parameters as tlcscribcd in Figure **3.** The dashed line is the behavior expected for a single ferromagnetic layer Tlie iiisct figure shows the hysteresis of tlic resonance frequency in tlic vicinity of tlic spin-flop field.

Iii rcgioii I:

$$(\frac{\omega}{\gamma})^2_{\pm} = H_0^2 - H_D^2 + (H_D + H_{ex})(2H_D - H_u) \pm [H_0^2(2H_D - H_u) \times (2H_D - H_u + 4H_{ex}) + H_{ex}^2 H_u^2]^{1/2} . \quad (25)$$

In rcgioii II:

$$\left(\frac{\omega}{\gamma}\right)^2_{\pm} = [2H_{ex}^2 + H_D(H_{ex} - H_u)]sin^2\theta + (H_{ex} - H_u)(H_{ex} - H_D) - H_{ex}^2 \pm H_{ex}[(2H_{ex} - 2H_u + H_D)sin^2\theta - (H_D - H_u)] , \quad (26)$$

where $sin\theta = H_0/(2H_{ex} - H_D)$.

In region III

$$(\frac{\omega}{\gamma})^2_{\pm} = (H_0 + H_D - H_{ex} \pm H_{ex})(H_0 - H_u + H_D - H_{ex} \pm H_{ex}) \quad (27)$$

When tlic field is applied normal to tlie film, $\mathbf{H}_0 \parallel$ y-axis, tlic dispcrsioii rclatioii is shown iii Figurc 5. Iii region I tlie acoustic modc maintains its Iiigli frequency status while tlie optical mode is at low but finite frequency. The shift of tlic tlie optical mode from zero is due to tlic weak in-plane aiiisotropy field, H_D. At saturation aiid in rcgioii 11, Llic acouslic iiiodc is again degenerate with llic normal ferromagnetic resonance aiid tlic optic mode remain at a ficld, $2H_{ex}$, higher than that of tlic acoustic iiiodc as expressed by tlic equations:

Iii rcgioii I:

$$(\frac{\omega}{\gamma})^2_{\pm} = -H_{ex}^2 cos2\phi + (H_{ex} + H_D)[H_{ex} + (H_D - H_u)cos^2\phi] \pm \{H_{ex}[H_{ex} + (H_D - H_u)cos^2\phi - (H_{ex} + H_D)cos2\phi\} , \quad (28)$$

where $sin\phi = H_0/(2H_{ex} + H_D - H_u)$.

In rcgioii II:

$$(\frac{\omega}{\gamma})^2_{\pm} = (H_0 + H_u - H_D - H_{ex} \pm H_{ex})(H_0 + H_u - H_{ex} \pm H_{ex}) \quad (29)$$

As opposed to tlic case for parallel coupling between tlic layers, for anti-parallel coupling tlie optical iiiodc is observed at lower frequencies. Sliis shift to lower frequencies is duc to tlic decrease iii tlic exchange ciicrgy as tlie magnetizations iii tlic tiro layers deviate from tlic parallel orientation as opposed to tlic increase in ciicrgy for tlic parallel coupled case, $A_{12} > 0$. Tlius in tlic CFFR experiments, tlic low field mode should have tlic stronger absorption while tlie Iiigli field modc, tlic optic mode, will have zero iiitciisity for identical layers aiid a weak iiitciisity if tlic layers have small difference in cither M or their internal ciicrgy.

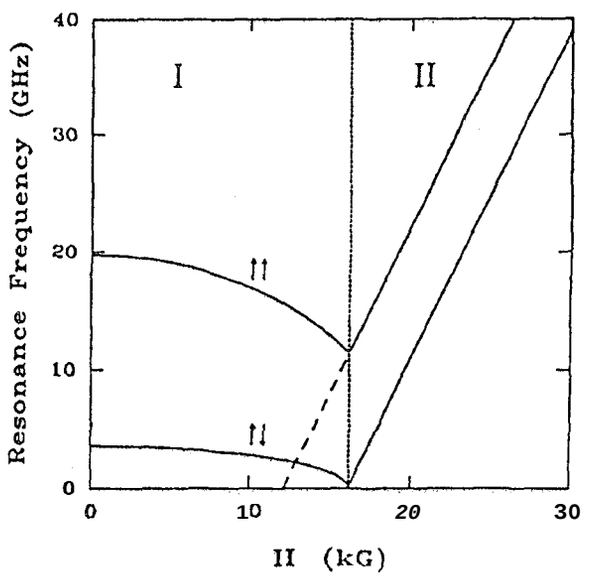

Figure 5: Tlic dispcrsioii rclatioii for tlic same condition as Figure 5 with tlic exception that tlie magnetic field is applied normal to tlic plane of tlie film. Again tlic dashed line is tlic dispersion curve prcdictcd for tlie single ferromagnetic layer.

11.4 Multilayer Films

In a system with N ferromagnetic/"non-magnetic" periods, the dispersion relations can be obtained from Eq. (6). Assuming that the N ferromagnetic layers are identical and the exchange coupling coefficients between each adjacent layers are the same, $A_{i,i\pm1} = A_{12}$, the system will have N normal modes whose "wave function" will vary sinusoidally across the film layers and have a natural boundary condition (zero slope) at the surface of the structure. The "fundamental mode" for this set of boundary conditions will have all the ferromagnetic layers precessing in phase with the same amplitude, the uniform mode.

In the case of parallel coupling between the layers, the high order spin wave modes will occur at the high frequency or low magnetic field side of the uniform mode. The highest frequency or lowest field mode, will correspond to that of the optic mode discussed in the trilayer system with the rf magnetization precessing anti-parallel to each other between the ith and $(i\pm1)$th layer. In the saturation region, tlie field separation between the optic mode and the uniform mode is in the range of $2H_{ex} \leq \Delta H_{res} \leq 4H_{ex}$, with $\Delta H_{res} = 2H_{ex}$ for N = 2 and ΔH_{res} approaching $4H_{ex}$ when the number of periods approaches infinity.

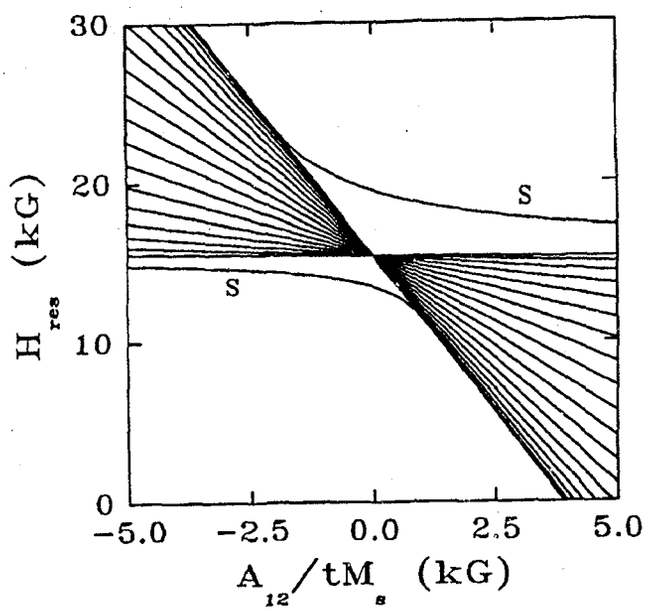

Figure 6: The spin-wave resonance modes for a set of 20 periods of magnetic/"non-magnetic" layers as a function of the strength of the exchange interaction when the field is applied normal to the film. The values of the parameters used are $H_{u,1} = -16$ kG, $H_{u,i} = -12$ kG where i = 2, ..., 19, $H_{u,20} = -10$ kG and $\omega/\gamma = 3.5$ kG. The "surface" like modes are labeled with a "S".

In the case of anti-parallel coupling between the layers, the N normal modes will again lie between the values of the uniform mode (or acoustic mode) and the optical mode. However, in the saturation region, tlie high order spin wave modes will occur at tlie low frequency or high field side because the out of phase rf magnetization resonance will reduce tlie interlayer exchange energy.

For all but tlie uniform mode, tlie precession of each layer will have a systematic variation of amplitude and phase from layer to layer such that tlie net transverse rf dipole moment of these modes will be zero and tlierefore will not not be excited by a uniform rf field.

In many instances, the surface ferromagnetic layers will have a different environment due to the broken symmetry. As a result, the energy expressions for $\mathcal{E}_1$ and $\mathcal{E}_N$ rnay be quite different from those in tlie "bulk" of tlie structure. Depending on the nature of $\mathcal{E}_1$ and/or $\mathcal{E}_N$, a pinned or unpinned [13,29] boundary may exist. For a pinned boundary condition, tlie lowest order mode will be a sinusoidal mode for parallel coupling ($A_{12} > 0$) while it will have an exponential "surface" like mode for anti-parallel coupling ($A_{12} < 0$). For an unpinned boundary condition, the "surface" like mode can only be observed in the parallel coupled multilayer system. Figure 6 shows tlie resonance fields as a function of the exchange field, A_{12}/tM, at X-band, $\omega/\gamma = 3.5$ kG, with the applied field normal to the film for a 20 periods multilayer film. The film is assumed to have an unpinned boundary condition in the first layer and a pinned boundary condition in the 20th layer.

These results sliow that CFFR spectra can be a very sensitive probe of the internal energies of each layer as well as the interlayer exchange coupling strength.

III. Experimental Results

CFFR experiments have been carried out on many multilayer systems with the structure $(TM/NM)_N$, where TM is tlie ferromagnetic transition metal layer such as Co, Fe, Ni or their alloys and NM is tlie "non-magnetic" metal such as Pt, Pd, Cr, Cu, Ag, Ru and Au. The research has concentrated on the internal anisotropy energy within eacli magnetic layers and tlie interlayer exchange coupling as a function of both the magnetic layer thickness and tlie "non-magnetic" layer thickness. Temperatnre dependente of those properties has also been studied.

111.1. Interna1 Anisotropy Energies

The internal energies having the form expressed by Eq. (8) through (15) have been determined for a number of structured systems by the study of angular dependente of the CFFR spectra. The cubic crystalline anisotropy energy, showing a 4-fold anisotropy energy in the film plane, can be observed in some of tlie MBE grown single-crystal samples. A typical resonance field as a function of the orientation of the externa1 field within the field plane is shown in Figure 7. Heinrich, *et al.*[7,19,23,30,31] determined the cubic crystalline anisotropy energy constants K_1 for several systerns

such as Fe(001)/Ag(100), Ni(001)/Fe(001)/Ag(001), Co(001)/Cu(001) and Fe(001)/Cu(001)/Fe(001). In tlie case of single crystal Fe layer deposited on Ag substrate, K_1 decreases draniatically from tliat of tlie bulk Fe value wlicn Fe layer tliickness is less tlian 10 Å. Tlie deposition of an extra Ni overlayer (> 6 monolaycr) on top of tlie Fe layer enhanced tlie cubic crystalline anisotropy energy by an order of magnitude due tlie lattice reconstruction in tlie Fe/Ni bilayers. Similar effects lias not been found if tlie Ni layer is replaced by Cu. A negative value of tlie cubic anisotropy field, $2K_1/M$, was observed to be about -1 kG in tlie Co(001)/Cu(001)/Co(001) structures. Tlie cubic anisotropy energy increases witli tlie decrease of temperature and nearly double tlie room temperature value at 77 K.

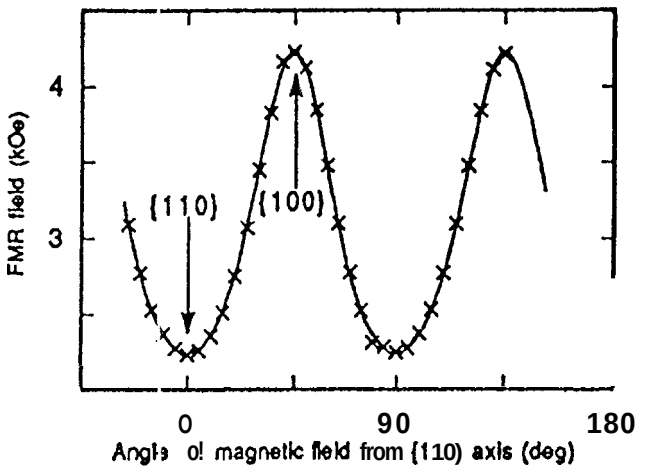

Figure 7: In-p ane angular dependence of the FMR field observed for the $(Co)_{4\,3}/(Cu)_6/(Co)_4$ saniple, where tlie subscript is in monolayers. Tlie solid line represents a theoretical fit using tlie following magnetic values: $H_u = -40.8$ kG, $2K_1/M = -1.05$ kG, f = 36.3 GIIz, and $g = 2.16$. (from Ref. 30)

In a 40 Å Fe(001)/Cr(001)/40 Å Fe(001) structure, Krebs et *al.*[25,32] observed as many as five resonance modes at some microwave frequencies with the external field applied along the [1$\bar{1}$0] direction in the film plane. The ccmplex spectra were explained using tlie cubic anisotropy energy along with the interlayer excliange coupling between tlie two Fe layers as sliown in Figure 8. It was reported tliat the cubic anisotropy field, $2K_1/M$, is independent of the Cr tliickness in the range $12\mathring{A} < t_{Cr} <$ 25A and tlie values are close to tliat of tlie bulk Fe.

The dominant term in the CFFR spectra is tlie effective uniaxial anisotropy energy normal to tlie film, including tlie demagnetization energy, tlie internal bulk uniaxial anisotropy energy and the surface anisotropy energy as expressed in Eq. (12) and (13). From a series of 275 Å Ag/Fe/550 Å Ag structures for Fe layer thickness of 24 Å, 48 Å and 80 Å, Hurdequint, et *al.*[15] determined tlie surface anisotropy energy, K_{sur}, between eacli Fe/Ag interface to be 1.05 erg/cm^2. In a $(Fe/Pt)_N$ multilayer structure where N=35 or 50, Wigen, et *al.*[16] reported a surface anisotropy energy of 0.14 erg/cm^2 for tlie Fe tliickness of 5 Å, 7 Å and 15 Å with Pt tliickness constant at 15 Å. Purcell, et *al.*[17] investigate the internal field for Co/Pd(111) structures for which a 9 monolayer film of Pd was deposited on Co layers tliat varied from 5 to 12.5 monolayers. The observed value of K_{sur} was found to be 0.8 erg/cm^2.

Zhang, et *al.*[18,29] investigated the development of the induced uniaxial anisotropy energy as a function of tlie Pt thickness in Co/Pt multilayer films. For a series of Co/Pt structure having 20 periods, tlie Co layers were 25 Å thick and tlie Pt layers varied from 1 Å to 18 Å. Tlie evolution of tlie anisotropy energy was observed to depend on tlie tlie Pt interlayer tliickness as

$$K_{2u} = K_{2u}^b + \frac{2K_{sur}^0}{t_{Co}}[1 - exp(-\frac{t_{Pt}}{t_0})] . \qquad (30)$$

The exponential term accounts for tlie dependence of the surface anisotropy energy on the thickness of the Pt layer. Tlie value of t_0 is 13 Å and the value of surface anisotropy energy, K_{sur}^0, for this Co/Pt structure is 0.91 erg/cm^2.

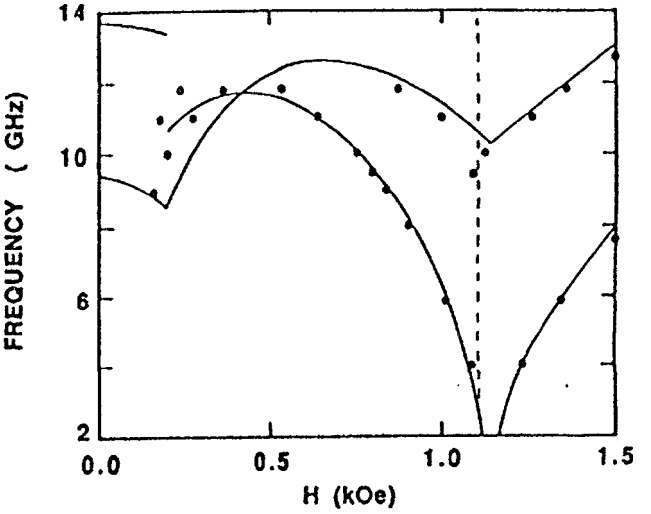

Figure 8: Multiple-frequency FMR data for tlie (40 Å Fe/13 Å Cr /40 Å Fe) tliin film sample witli tlie external field parallel to tlie hard axis in tlie film plane [1$\bar{1}$0]. Tlie solid curves are tlie result of resonance mode calculations using tlie following parameters: $H_K = 2K_1/M = 520$ G, $A_{12}/tM = -300$ G and $H_D = 2D/M = 10$ G. The dashed line marks the saturation field. (from Ref. 25)

The contribution from the surface anisotropy energy will become larger than tliat of tlie magnetostatic energy when tlie thickness of the magnetic layer decreases to a critical value, t,,. For films with the magnetic layer thinner than t_{cr} a perpendicular magnetic anisotropy

property, $K_{2u}^{eff} > 0$, will be obtained and tlie magnetization will be oriented normal to tlie film. In Co/Pt and Co/Pd multilayer structures[17,18], tlie traiisition thickness is about $10 \sim 15$Å.

Artman, *et al.*[33] measured the angular dependence of tlie CFFR in a number of Co/Pt niultilayer films and obscrvcd that tlie fourth order uniaxial anisotropy energy constant, K_{4u}, as exprcssed in Eq. (11), cannot be neglccted in the system when tlie second order term K_{2u}^{eff} is close to zero. Over a series of sevcn different Glms liaving various tliicknccsscs of tlie Co and tlie Pt, tliere appcared to be no consistent variation in tlie values of tlie fourth order anisotropy field, $4K_{4u}^{eff}/M$, which is in tlic range of $0 \sim 1$ kG.

111.2. Iiitcrlayer Excliange Coupling

Tlie important difference between tlie coupled niultilaycr system and tlie single layer system is tlie existence of tlie exchange modes. The advantage of using CFFR and Brillouin light scattcring is tlie ability to observe tlie excliange modes predicted in tlie previous section and to evaluate tlie sign and magnitude of tlic excliange coupling constant, $A_{i,i+1}$. Those exchange modes have been obscrved in many multilayer systems sucli as Fe/Cr[1,2,12,25,32], Fe/Cu[7,31,34–36], Fe/Ag[19,36], Fe/Au[12,36], Fe/Pd[9,35–37], Fe/Pt[16], Fe/C[38], Co/Cu[30], Co/Pd[8,10], Co/Pt[18,29,39], Co/Ru[27,40], Ni_xFe_{1-x}/Cr[11,41], Ni_xFe_{1-x}/Cu[11,41,42], Ni_xFe_{1-x}/Pd[11,41] and Ni_xFe_{1-x}/Ag/Ni[11,43].

As mcntioned before, tlie iiiterlayer laycr exchange coupling constant, A_{12}, is proportional to tlie resonance field separation of the acoustic mode and tlie optical mode, ΔH_{res}, in a system witli two ideiitical magnetic laycrs separated by tlic "non-magnetic" layer. Hoivever tlie optic mode can not be observcd in tlie CFFR spcctra unlcss a difference of the effective uniaxial anisotropy ficld, ΔH_{2u}^{eff}, is created between tlie two magnctic laycrs. As a result, the separation bctween the two rnodcs, $\Delta H_{res}(A_{12}, \Delta H_{2u}^{eff})$, does not only depend on tlie interlayer excliange coupling constant but also on tlie difference of tlie effective uniaxial anisotropy field. A_{12} can be obtained when ΔH_{2u}^{eff} is known or if it is so small compared with the exchange field, $2A_{12}/tM$, that it can be neglected. The former condition can be acliieved by making two separated single layer films witli similar structure as that in the trilayer system and measure the internal anisotropy energy for each films. Tlie latter condition will be satisfied if tlie intensity of tlie acoustic mode is at least an order of magnitude larger than that of the optical mode. Otherwise the iiitensity expressed in Eq. (17) as well as tlie resonance fields must be used to calculate A_{12} properly. In a multilayer structure with N > 2, the exchange constant, $A_{i,i\pm1}$ can be evaluated from tlie field or frequency dependence of tlie "spin-wave" like higher order exchange modcs.

Of tlic systcrns investigated to date, Pt and Pd interlayers have a positive exchange coupling constant producing a parallel coupling between tlie ferromagnetic layers for all values of tlie tliickness. Bloemen, *et al.*[39], invcstigatcd the trilayer films of Co/Pt/Co with tlie Pt laycr tliickness varied from 4 Å to 100 Å. Tlie tliickness of tlie Co laycrs are 50 Å and 20 Å respectivcly so as to produce an anisotropy difference in each Co layer. Tlic effective anisotropy fields for each laycrs were chosen to give a best fit of tlic resonance fields for a total of 8 samplcs. Tlie in-pliasc and out-of-phase modcs can bc obscrved only in films witli Pt layer thicknccss greater than 20 Å. The exchange constaiit A_{12} was found to decrease with tlie increase of tlie Pt tliickncss as shown in Figure 0.

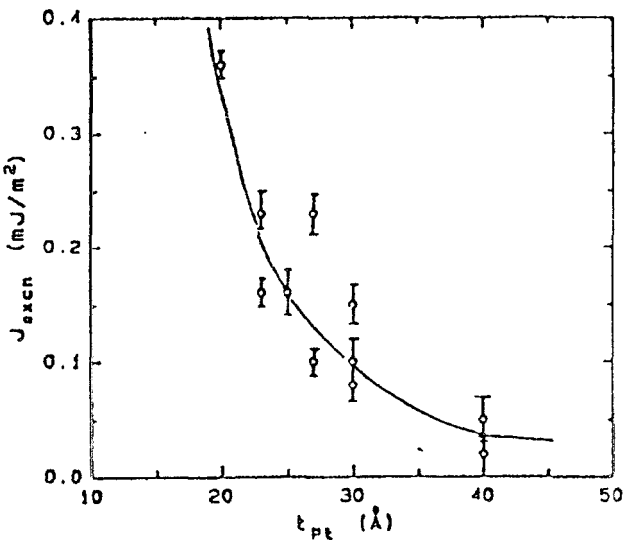

Figure 0: Interlayer excliange energy J_{exch} (tlic same as A_{12}) as a function of tlic Pt spaccr thickness. (from Rcf. 39)

In a scrics of $(Co/Pt)_{20}$ structures investigated by Zliang, *et al.*[18,29], tlie first Co layer of tlic structurc was dcposited on a Ru buffer laycr. Tliis removes one of tlic Pt interface contributions to tlie uniaxial anisotropy energy il1 layer one, wliicli depends on tlie Pt tliickncss and is on tlie order of 5 kG for $t_{Pt} \geq 10$ Å. As a result tlie effective anisotropy energy in layer one is different from tliose of bulk layers as tlie Pt layer develops. Tliis produces an unpinned surface coiidition with tlie externa1 field normal to tlie film. Two modes, tlie "surface like" mode aiid tlie first order spin-wave excliange mode, were observed for tlie films witli Pt tliickncss greater than 4 Å. From tlie analysis of tlie positions and intensities of the modes in tlic CFFR spectra it was possible to determine tlie excliange coupling coefficient as a function of tlie Pt tliickness in tlie range of $4Å \leq t_{Pt} \leq 18Å$. The relation was found to have an exponcntial depeiidence

$$A_{12}(t_{Pt}) = A_{12}^{0} \exp\left(-\frac{t_{Pt}}{\xi}\right), \qquad (31)$$

where A_{12}^0 was measured to be 70 erg/cm^2 and t_0 to be 7 Å for this series.

Bosse, *et al.*[41] investigated two permalloy ($Ni_{80}Fe_{20}$) films separated by different "non-magnetic" layers such as Pd, Cu, and Cr. The exchange coupling across Pd and Cu follows the same exponential relation as expressed in Eq. (30). with a greater decay length for Pd.

Celinski, et *al.*[37] studied a series of Fe/Pd/Fe trilayer films grown by MBE. A weak optical mode was observed in films with the Pd thickness greater than 5 monolayer. The exchange coupling constant evaluated from the resonance fields reveals an oscillatory behavior superimposed on the exponential decreasing background. The oscillation period, 4 monolayer, is larger than that predicted from the layered RKKY interactions.[44]

In contrast to Pt and Pd, the metals such as Cu, Ag, Au, Cr, and Ru produce exchange coupling coefficients that oscillate between positive and negative values to produce parallel or anti-parallel coupling between the magnetic layers as a function of the thickness of the "non-magnetic" layer. In a Fe/Cr/Fe trilayer structure for which the Fe layers were 110 Å and the Cr varied from 2 to 20 Å, Barnas, *et al.*[12] determined the sign and magnitude of the exchange coupling constant from the positions of the two resonance frequencies in the Brillouin light scattering spectra, taking into account the exchange energy within each Fe layer as well. The interlayer coupling changes sign from parallel coupling at $t_{Cr} < 7Å$ to anti-parallel coupling at $t_{Cr} > 7$A. The coupling coefficient vanishes at $t_{Cr} \approx 17Å$. Using CFFR technique, *Krebs*, et *al.*[25], investigated another Fe/Cr/Fe series for which the Fe layer was 40 Å thick and the Cr varied from 4 to 85 Å. Multimodes were found in the resonance spectra that were consistent with anti-parallel coupling for Cr thickness between 13 Å and 24 Å. A maximum exchange field of about 300 G was obtained at $t_{cr} \approx 16Å$. No antiferromagnetic alignment was shown in both the $t_{Cr} < 13$ Å region and the $t_{Cr} < 24$ Å region.

In a series of Fe/Cu, Ag, Au/Fe trilayer structures, Celinski, et *al*[36], observed an oscillation from parallel to anti-parallel coupling as a function of the Cu thickness with a periodicity of ~ 10 monolayer. The amplitude of the coupling constant decreases with increasing Cu thickness and the values at 77 K are almost double those at room temperature. The oscillations in the Ag and/or Au included structures were much weaker compared with those of Fe/Cu/Fe structures and the coupling constant decreases rapidly to zero as the thickness exceeds 6 to 10 monolayers.

Zhang, et *al.*[40] have investigated Co/Ru/Co trilayers and for Ru layer thicknesses on the order of 10 Å, a very strong ant -parallel coupling between the Co layers is observed for which the acoustic mode and the optic mode could be separated by as much as 4000 G. These

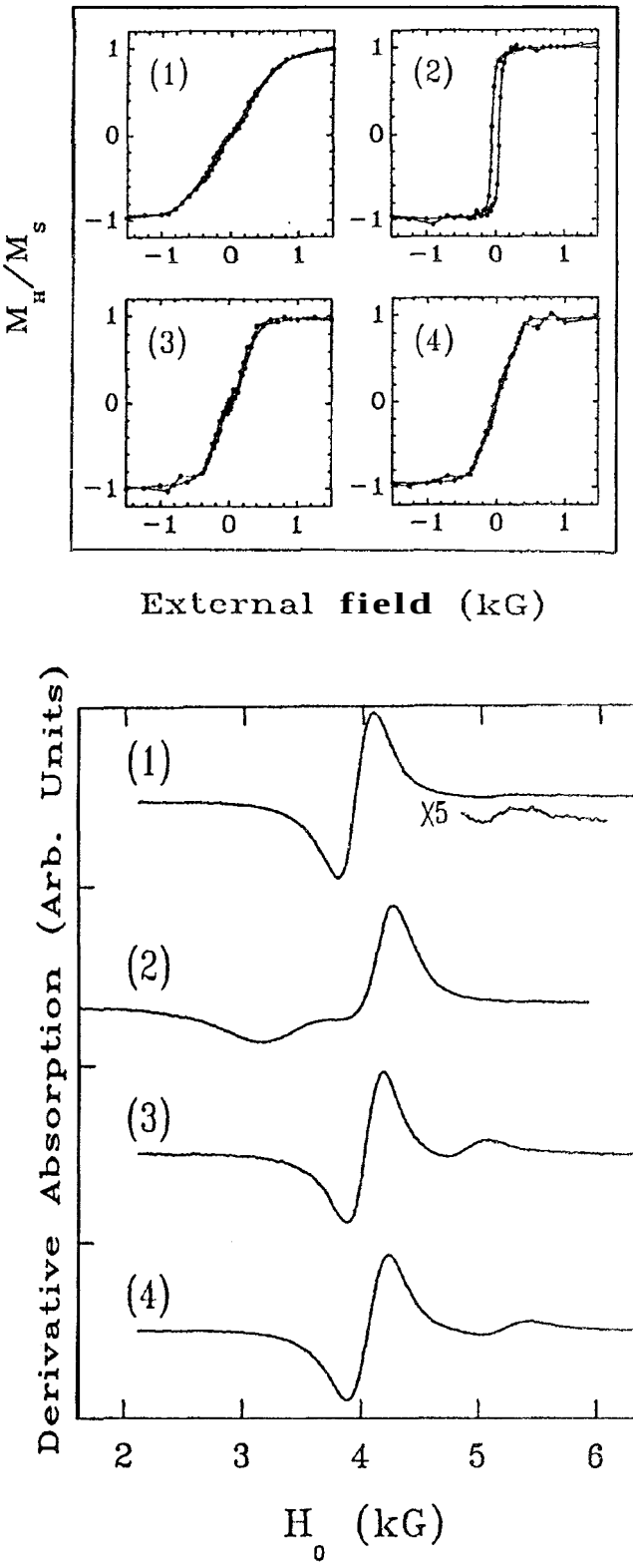

Figure 10: top) In-plane magnetization measurement as a function of the field strength for the structure of (32 Å Co/Ru/32 Å Co) trilayers. The Ru thicknesses are (1) 15 Å, (2) 20 Å, (3) 25 Å and (4) 30 Å. bottom) CFFR spectra at 22.9 GHz with the magnetic field applied in the film plane. The samples are the same as those mentioned in part a). (from Ref. 40)

values are about an order of magnitude larger tlian that observed in tlie other typical structures. Tlie spectra as well as the magnetization hysteresis loop lias clearly shown an oscillation behavior of tlie coupling coiistant from positive to negative witli tlie change of Ru thickness (see Figure 10).

Tlie temperature dependence of tlie excliange coupling coiistant, A_{12}, for a Fe/Pd/Fe structure lias beeii studied by Heinrich, et *al.*[9]. A_{12} increases with tlie decrease of temperature, followiiig a Curie-Weiss type of dependence

$$A_{12} \propto 1/(T + \Theta) \tag{32}$$

with Θ on tlie order of 50 K.

111.3. Miscellaneous Effects

Hurdequint, et *al*[45], investigated the line shape aiid relaxation processes in Fe/Ag multilayer structures. For tlie in-plane or parallel orientation for CFFR resonance tlie ratio of tlie slopes of the absorbtion line of tlie liigli field to the low field side of tlie line, A/B, was found to vary between 0.7 aiid 1.0 for tlie whole series for films. Tliis corresponds to a positive signal phase and tlie effect cannot be explained by tlie eddy current contributions for wliicli tlie A/B, ratio should be grealer than unity. Tlie details of tlie mechanism responsible for this effect remains to be explained. The linewidth of tlie resonance modes were consistent with a mechanism in wliicli tlie magnetic energy is carried away (relaxed) by tlie conduction electrons. In Ag, the spin diffusion length would have a value $\delta_{eff} = (2DT_2)^{1/2}$, with D the electron diffusion coiistant and T_2 tlie transverse spin relaxation time. From tlie analysis a diffusion lengtli of 500 to 1000 Å is determined whicli is in reasonable agreement with results obtained by other techniques in Ag metals.

Heinrich, et *al.*[23], observed that tlie linewidth of tlie CFFR spectra as a function of the resonance frequency for a MBE grown Ni/Fe bilayer structure with a large 4-fold in-plane anisotropy energy follows the relation

$$\Delta H_{res} = \Delta H_0 + A\omega \,, \tag{33}$$

where ΔH_0 originates in tlie inliomogeneitics of the sarnple and the frequency dependent part is caused by the intrinsic Gilbert damping as expressed in Eq. (16). The damping related parameter A was nearly isotropic while ΔH_0 was sensitive to the direction of tlie external field. ΔH_0 was almost four times larger with tlie external field along the hard direction in tlie film plane than that with the external field along the easy axis. This was explained to be a result of crystalline defects generated during the Ni overlayer lattice relaxation. In another structure with a single Fe(100) film grown on Ag(001) substrate[19], the same group reported a rapid increase, almost an order of magnitude, in the Gilbert damping coefficient with decreasing Fe thickness from 40 Å to 4Å. Enhanced spin-orbit coupling for thinner Fe films was proposed to be tlie reason for tlie increase of tlic Gilbert damping parameter.

IV. Conclusions

Tlie magnetic properties of tlie magnetic/"non-magnetic" multilayer structures have been widely studies by the CFFR teclinique. Tlie intrinsic niagnetic parameters, sucli as tlie internal uniaxial anisotropy energy and tlie exchange coupling coiistant, varied from oiie series to another depending on tlie structure of tlie sample, tlie tliickness of eacli layer and tlic sample preparation coiiditions. While it is not possible to "catalog" all of tlie results in a convenient form, there are a few generalities that can be proposed.

(1) In most of tlie structures, tlie internal uniaxial anisotropy energy of tlie magnetic layer is significantly modified from tliat of tlie bulk materials as its tliickncss is reduced to tlie order of 10 Å. One of most important contributions to this cliange is due to the surface anisotropy energy developed from tlic interface interaction between tlie magnetic layer aiid "non-magnetic" layer which can be expressed as an effective anisotropy energy to tlie bulk of tlie niagnetic layer sucli tliat

$$K_{eff} = K_{sur}/t \,, \tag{34}$$

where t is tlie tliickness of tlie magnetic layer. Typical values of tlie surface anisotropy energy coiistant, K_{sur}, vary from 0.1 to 1 erg/cm^2, having a preferred orientation of tlie magnetization normal to tlie film. A transition tliickmss t_{cr}, below which tlie internal uniaxial anisotropy energy will dominate tlie magnetostatic aiiisotropy energy to produce an easy axis normal to tlie film, exists when tlie values of tlie magiietic layer tliickncss varied from 2 to 10 monolayers in most of tlie systems. Tlie origin of tlie surface anisotropy energy may come from tlie Néel surface anisotropy energy[46], tlie niagnetostriction energy, tlie interlayer diffusion or tlie polarization of tlie "non-magnetic" surface atoins.

(2) One of tlie most important contributions of tlie CFFR teclinique to tlie understanding of tlie magnetic properties of multilayer systems is tlie evolution of the interlayer excliange coiistant, A_{12}. For Pt aiid Pd interlayers, tlie coupling coefficient is positive producing parallel alignment of tlie magnetization of tlie layers. The coupling strength decreases with tlie increase of tlie "non-magnetic" lnyer tliickness t_{NM} following rouglily an exponential form

$$A_{12} = A_{12}^0 \exp(-t_{NM}/t_0) \,, \tag{35}$$

for wliicli the decay lengtli t_0 is on tlie order of 10 Å and A_{12}^0 is on tlie order of 1 to 50 erg/cm^2, about an order of magnitude smaller than tlie dircct excliange interactions within tlie magnetic layers.

For Cr, Cu and Ru interlayers, tlie coupling coefficient oscillates from positive (parallel coupling) to negative (anti-parallel coupling) while tlie amplitude of tlie

oscillation decreases as a function of the thickness. The oscillation period was observed to be on the order of 10 Å to 15 Å.

The variation of the exchange interaction through "non-magnetic" layers is similar to the polarization of the host material by the nearby 3d-transition magnetic atoms in a dilute transition metal alloy system. The bare magnetic moment of the dissolved 3d-atom in this system, polarizes its surroundings, and the polarization, as a function of the distance, is governed by the generalized magnetic susceptibility of the host material. If the host material were a normal metal in which the conduction electrons can be treated as free electrons, like in Cu and Ag, this susceptibility $\chi(r)$ will oscillate from positive to negative following the RKKY formula[47]. However if the intra-atomic exchange interactions between the band electrons in the host metal are important, like in Pt and Pd, the susceptibility will differ from the RKKY form and roughly follows an exponential decay form:[48]

$$\chi(r) \propto \frac{1}{r} \exp(-r/r_0) \,. \qquad (36)$$

This might explain the fact that no oscillation were found in the Ft and Pd included multilayer systeins although the mechanism of the interaction through "pinholes" in the Pt or Pd layers, is another possibility. The oscillations in the exchange interaction, A_{12}, observed in noble metal interlayers, suggest that a RKKY type interaction plays an important role in the multilayer exchange interaction. However the oscillation period in the Cu included multilayer system is significantly larger than that predicted from the layered RKKY calculation[44]. There is no well known mechanism that accounts for the observed beliavior of the coupling mechanism for this structure though a surface roughness model[49] was proposed to explain the long period oscillations to some extent. In Cr and Ru, the conduction electrons band structures are more complicated than that in the noble metal. They can not be treated using the free electron model. A successful theory must include the details of the band structures near the Fermi surfsces in these "non-magnetic" layers[50].

As more combinations of coupled magnetic/"non-magnetic" structures are developed and investigated, it is likely that additional new effects will be observed as well as a class of materials having a wider range of variables than those observed to date. It is expected that such structures will have a variety of useful applications that depend on microstructural properties. At present two such applications include magneto-optical storage media and magnetic readheads for computers.

References

1. P. Grunberg, R. Schreiber, Y. Pang, M. B. Brodsky, and H. Sowers, Phys. Rev. Lett., 57, 2442 (1986).
2. F. Saurenbacli, U. Walz, L. Hinchey, P. Grunberg, and W. Zinn, J. Appl. Phys. 63, 3473 (1988).
3. S. S. P. Parkin, N. More, and K. P. Roche, Phys. Rev. Lett., 64, 2304 (1990).
4. G. Binasch, P. Grunberg, F. Saurenbach, and W. Zinn, Phys. Rev. B, 39, 4828 (1989).
5. P. F. Carcia, A. D. Meinhaldt, and A. Suna, Appl. Phys. Lett. 47, 178 (1985).
6. W. B. Zeper, F. J. A. M. Greidanus, P. F. Carcia, and C. R. Finclier, J. Appl. Phys. 65, 4971 (1989).
7. J. F. Cochran, J. Rudd, W. B. Muir, B. Heinrich, and Z. Celinski, Phys. Rev. B, 42, 508 (1990).
8. B. Hillebrands, J. V. Harzer, G. Guntlierodt, C. D. England, and C. M. Falco, Phys. Rev. B, 42, 6839 (1990).
9. Z. Celinski, B. Heinrich, J. F. Cochran, W. B. Muir, A. S. Arrott, and J. Kirschner, Phys. Rev. Lett., 65, 1156 (1990).
10. B. Hillebrands, J. V. Harzer, and R. L. Stamps, G. Guntlierodt, C. D. England, C. RI. Falco, J. Magn. Magn. Mater., 93, 211 (1991).
11. M. Vohl, J. Barnas, and P. Grunberg, Phys. Rev. B, 39, 12003 (1989).
12. J. Barnas, aiid P. Grunberg, J. Magn. Magn. Matcr., 82, 186 (1989).
13. P. E. Wigen, Thin Solid Films, 114, 135 (1984).
14. A. Layadi, and J. O. Artman, J. Magn. Magn. Mater., 92, 143 (1990).
15. H. Hurdequint, J. Magn. Magn. Mater., 93, 336 (1901).
16. P. E. Wigen, Z. Zhang, S. Iwata, and T. Suzuki, J. Magn. Soc. Jpn., Supp. S1, 15, 33 (1991).
17. S. T. Purcell, II. W. van Kesteren, E. C. Cosman, W. B. Zeper, and W. Hoving, J. Appl. Phys., 69, 5640 (1991).
18. Z. Zliang, P. E. Wigen, and S. S. P. Parkin, J. Appl. Phys., 69, 5649 (1991).
19. B. Heinrich, K. B. Urquhart, A. S. Arrott, J. F. Cochran, K. Myrtle, and S. T. Purcell, Phys. Rev. Lett., 59, 1756 (1987).
20. J. Barnas, Phys. Rev. B, 45, 10427 (1992).
21. B. Hillebrands, Phys. Rev. B, 37, 9885 (1988).
22. B. Hillebrands, Phys. Rev. B, 41, 530 (1990).
23. B. Heinrich, S. T. Purcell, J. R. Dutcher, K. B. Urquhart, J. F. Cochran, and A. S. Arrott, Phys. Rev. B, 38, 12879 (1988).
24. H. Puszkarski, Acta Phys. Pol. A, 38, 899, (1970).
25. J. J. Krebs, P. Lubitz, A. Chaiken, and G. A. Prinz, J. Appl. Phys. 67, 5920 (1990). J. J. Krebs, P. Lubitz, A. Chaiken, and G. A. Prinz, Phys. Rev. Lett., 63, 1645 (1989).
26. B. Dieny, and J. P. Gavigan, J. Phys., 2, 159, 187, (1990).

27. K. Ounadjela, D. Muller, A. Dinia, A. Arbaoui, P. Panissod, and G. Suran, Pliys. Rev. B, 45, 7768 (1902).
28. S. Foner, *Magnetism*, Ed. by G. T. Rado, and H. Sulil, (Academic Press, New York, 1963) Vol. I, p383.
20. Z. Zhang, P. E. Wigen, MORIS'92 (Tucson, Arizona, 1092).
30. B. Heinrich, J. F. Cocliran, RI. Kowalewski, J. Kirschner, Z. Celinski, h. S. Arrott, and K. Myrtle, Phys. Rev. B, 44, 9348 (1991).
31. B. Heinrich, Z. Celinski, J. F. Cocliran, TV. B. Muir, J. Rudd, Q. RI. Zhong, A. S. Arrott, K. Myrtle, and J. Kirschner, Pliys. Rev. Lett., 64, 673 (1990).
32. J. J. Krebs, P. Lubitz, A. Cliaiken, aiid G. A. Prinz, J. Appl. Pliys., 69, 4795 (1991).
33. J. O. Artman, D. J. DeSmet, X. Shao, J. C. Cates, C. Alexander, Jr., RI. R. Parker, E. T. Lacey, D. G. Lord, and P. J. Grundy, J. Appl. Pliys., 70, 6038 (1991).
34. A. Layadi, and J. 0 . Artman, J. Appl. Pliys., 64, 5760 (1988).
35. B. Heinrich, Z. Celinski, K. Myrtle, J. F. Cocliran, A. S. Arrott, aad J. Kirschner, J. Magn. Magn. Mater., 93, 75 (1991).
36. Z. Celinski, and B. Heinrich, J. Magn. Magn. Mater., 99, L25, (1991).
37. Z. Celinski, B. Heinrich, and J. F. Cocliran, J. Appl. Pliys., 70, 5870 (1991).
38. M. Pomerantz, J. C. Slonczewski, and E. Spiller, J. Appl. Pliys., 61, 3747 (1987).
39. P. J. H. Bloemen, E. A. M. van Alphen, TV. J. M. de Jonge, and E. J. A. den Broeder, 13th ICMFS, Glasgow, (1991).
40. Z. Zhang, P. E. Wigen, and K. Ounadjela, to be publislied.
41. H. Bosse, and H. Gartner, J. Magn. Magn. Mater., 80, 339 (1989).
42. J. S. S. Whiting, M. L. Watson, A. Chamber, I. B. Puchalska, H. Niedoba, H. O. Gupta, L. J. Heyderman, J. C. S. Levy, and D. Mercier, IEEE Trans. on Magn., 26, 2350 (1900).
43. A. Layadi, and J. O. Artman, J. Appl. Phys., 67, 4451 (1990).
44. Y. Yafet, Pliys. Rev. B, 36, 3948 (1987).
45. H. Hurdequint, and AI. Malouche, J. Magn. Magn. Mater., 93, 276 (1991).
46. L. Néel, Le Journal de Physique et le Radium, 15, 225, (1954).
47. K. Yosida, Phys. Rev., 106, 893 (1957); 107, 396 (1957).
48. J. A. Mydosh, and G. J. Nieuwenhuys, *Ferromagnetic Materials*, Ed. by E. P. Wohlfarth (North-Holland Publ. Co., Amsterdam, 1980) Vol. 1.
49. Y. Wang, and P. RI. Levy, Pliys. Rev. Lctt. 65, 2732 (1990).
50. D. RI. Edwards, J. Mathon, R. B. Muniz, and M. S. Phan, Pliys. Rev. Lett., 67 493 (1991).